Eur. Phys. J. C (2025) 85:298
https://doi.org/10.1140/epjc/s10052-025-14013-3

THE EUROPEAN PHYSICAL JOURNAL C

Regular Article - Theoretical Physics

Modified gravity/dynamical dark energy vs ΛCDM: is the game over?

Sergei D. Odintsov[1,2,6,a], **Diego Sáez-Chillón Gómez**[3,4,b], **German S. Sharov**[5,6,c]

[1] Institut de Ciències de l'Espai, ICE/CSIC-IEEC, Campus UAB, Carrer de Can Magrans s/n, 08193 Bellaterra, Barcelona, Spain
[2] Institució Catalana de Recerca i Estudis Avançats (ICREA), Passeig Luis Companys, 23, 08010 Barcelona, Spain
[3] Department of Theoretical, Atomic and Optical Physics, and Laboratory for Disruptive Interdisciplinary Science (LaDIS), University of Valladolid UVA, Campus Miguel Delibes, Paseo Belén, 7, 47011 Valladolid, Spain
[4] Department of Physics, Universidade Federal do Ceará (UFC), Campus do Pici, C.P. 6030, Fortaleza, CE 60455-760, Brazil
[5] Tver State University, Sadovyj per. 35, Tver 170002, Russia
[6] International Laboratory for Theoretical Cosmology, Tomsk State University of Control Systems and Radioelectronics (TUSUR), Tomsk 634050, Russia

Received: 28 January 2025 / Accepted: 27 February 2025
© The Author(s) 2025

Abstract Over the last decades, tests on the standard model of cosmology, the so-called ΛCDM model, have been widely analysed and compared with many different models for describing dark energy. Modified gravities have played an important role in this sense as an alternative to ΛCDM model. Previous observational data has been always favouring ΛCDM model in comparison to any other model. While statistically speaking, alternative models have shown their power, fitting in some cases the observational data slightly better than ΛCDM, the significance and goodness of the fits were not significantly relevant to exclude the standard model of cosmology. In this paper, a generalisation of exponential $F(R)$ gravity is considered and compared with ΛCDM model by using the latest observational data. Also some well-known model independent parameterisations for the equation of state (EoS) of dark energy are explored. These scenarios are confronted with the renewed observational data involving the Pantheon plus datasets of supernovae type Ia, the Hubble parameter estimations, data from the cosmic microwave background and baryon acoustic oscillations, where the latter includes the data provided by Dark Energy Spectroscopic Instrument Collaboration. Results of this analysis suggest that standard exponential $F(R)$ models provide much better fits than ΛCDM model, which is excluded at 4σ. Moreover, the parameterisations of the equation of state suggest a non-constant EoS parameter for dark energy, where ΛCDM model is also excluded at 4σ.

[a] e-mail: odintsov@ice.csic.es
[b] e-mail: diego.saez@uva.es (corresponding author)
[c] e-mail: sharov.gs@tversu.ru

1 Introduction

Modern cosmology aims to approach an exhaustive explanation of available observational data. To do so, many different approaches are followed in the literature. The Cosmological Standard model assumes General Relativity (GR) to be valid but at the price of assuming additional unknown components, such as dark matter, dark energy. Other well-known ways to explain the observations lies on considering different types of modifications of GR [1–6]. From time to time cosmologists have to improve the corresponding theories in order to achieve to describe new release of observational data.

Recent measurements of baryon acoustic oscillations (BAO) from the Dark Energy Spectroscopic Instrument (DESI) from Data Release 1 point to corrections in the predictions of some known cosmological models [7–9]. The DESI Data Release 1 includes BAO data from clustering of galaxies, quasars and the Lyman-α forest in the redshift range $0.1 < z < 4.16$. For some popular cosmological scenarios these new data in combination with the Pantheon+ compilation of type Ia supernovae (SN Ia) data [10] and other observational datasets can improve the estimations of the free model parameters, particularly the equation of state for dark energy, the Hubble constant as well as other parameters [7–9,11,12]. Moreover, new data, particularly late-time data, might help to infer about the solution to the Hubble constante tension [13], which seems to be eluded when one just considers early-time data [14].

In this paper, the new BAO and SN Ia observations are considered in the framework of modified gravity. In particular, the so-called $F(R)$ gravity, an extension of GR with a

Published online: 14 March 2025

Lagrangian that depends non-trivially on the Ricci scalar R is analysed. $F(R)$ gravity models have been widely analysed in the literature because they can successfully describe both the inflationary era and the late-time epoch with accelerating expansion of the universe [1–6,15]. In addition, some observational limitations that include local constraints, as in the Solar system, together with a reasonable limit to recover the usual cosmological evolution along radiation and matter dominated epoch have been analysed and some viable models that accomplish some particular constraints have been considered in the literature [16–20], which can also describe well the SN Ia, BAO, CMB observational data related to the late-time cosmological evolution [21–23].

One of the most interesting models of this type of viable $F(R)$ gravities is a class of exponential gravities [18,24–26]. These models contain a term that consists on a negative exponential of the Ricci scalar R, such that it mimics ΛCDM model asymptotically (at early times), when the exponential becomes negligible. Such scenario generally occurs in two cases: (a) as far as the Ricci scalar is large enough at the early epoch and/or (b) for a large value of the parameter that modulates the exponential. Indeed, when the Ricci scalar is below a particular scale, the exponential term plays an important role, and the resulting cosmological evolution can essentially differ from that predicted by the ΛCDM model. As shown previously in the literature, this type of exponential gravity can successfully describe observational data in comparison with other models [27–30]. Moreover, exponential gravities may reproduce the whole cosmological evolution, unifying early-time inflation and late-time acceleration. For this purpose an action should include an inflationary term (for example, based on R^2 inflation) that act effectively at early times but is suppressed or vanishes at the end of inflation [24–26,29]. Some modifications of exponential gravity with extra logarithmic terms motivated by quantum gravity and with an axion scalar field have been also studied and tested versus observational data in some previous papers [31–33]. Some other generalisations of exponential $F(R)$ gravity have been considered, where a term of the type $e^{f(R)}$ is included in the action [23,34,35].

In this paper, the standard exponential gravity model proposed in Refs. [18,24–26] is considered together with a generalisation of such a model. Both are tested with observational data and compared to ΛCDM model. Results of these tests strongly favour exponential $F(R)$ gravity models in comparison to ΛCDM model, even when considering the fact that the number of free parameters is larger for the $F(R)$ gravity cases. In this sense, ΛCDM model is excluded at more than 3σ for both exponential gravity models, reaching 4σ in the case of standard exponential gravity. Moreover, in order to check and support such results, some well-known model agnostic parameterisations for the dark energy equation of state (EoS) are considered, namely: wCDM and Chevallier–Polarski–Linder (CPL) models [36,37], where the former assumes a constant EoS parameter and the latter a dynamical one. Results also favour in this case a dynamical EoS for dark energy versus a constant one. Indeed, wCDM provides better fits than ΛCDM model, which lies within the 2σ confidence region i.e. with no statistically relevance, whereas CPL models fit much better the data and excludes ΛCDM at 4σ. These analysis confirm previous conclusions by some recent papers [7–9,38–43] where the recent DESI BAO data points to an evidence for modified gravity or dynamical dark energy. In addition, despite other older analysis also favoured the possibility of modified gravity [44], the evidence now turns out much stronger. Such an evidence is also supported by other different analysis where CMB anisotropy power spectra is studied [45]. Moreover, for long time the possibility that the EoS parameter deviates from -1 has been pointed out, also by some recent analysis [46], such that all these results support the idea that ΛCDM model might be ruled out definitely.

The paper is organised as follows: in Sect. 2, the dynamical equations for the exponential $F(R)$ gravity are obtained. In Sect. 3, SN Ia, BAO, $H(z)$ and CMB observational data are briefly described. The models are confronted with the observations and results are analysed in Sect. 4. In the next section we compare our $F(R)$ gravity tests with wCDM and CPL scenarios. Finally, conclusions are provided in Sect. 6.

2 Dynamics in $F(R)$ gravity

The so-called $F(R)$ gravity models are described by the following gravitational action: [18,24–29]

$$S = \int d^4x\sqrt{-g}\left[\frac{F(R)}{2\kappa^2} + \mathcal{L}_m\right], \tag{1}$$

where $\mathcal{L}_m$ is the matter Lagrangian, $\kappa^2 = 8\pi G$ with G being the Newtonian gravitational constant. Here, we are assuming a flat Friedmann–Lemaître–Robertson–Walker metric:

$$ds^2 = -dt^2 + a^2(t)\,\delta_{ij}dx^i dx^j\ . \tag{2}$$

Then, by varying the action (1), FLRW equations are obtained [29,32]:

$$\begin{aligned} 3H^2F_R &= \frac{RF_R - F}{2} - 3H\dot{F}_R + \kappa^2\rho\,,\\ -2\dot{H}F_R &= \ddot{F}_R - H\dot{F}_R + \kappa^2(\rho + p)\,. \end{aligned} \tag{3}$$

Here $F_R \equiv \frac{dF(R)}{dR}$, $H = \dot{a}/a$ is the Hubble parameter and the dot denotes derivatives with respect to the cosmic time t, whereas ρ and p are the energy density and the pressure for all the species (including dark matter and all the species), respectively. The continuity equation for the energy-momentum tensor takes the usual form:

$$\dot{\rho} = -3H(\rho + p) \,. \tag{4}$$

For the purposes of this paper, we might use the relation $R = 6\dot{H} + 12H^2$ to rewrite the FLRW equations (3) as a dynamical system as follows [29,33]:

$$\frac{dH}{d\log a} = \frac{R}{6H} - 2H, \tag{5}$$

$$\frac{dR}{d\log a} = \frac{1}{F_{RR}}\left(\frac{\kappa^2\rho}{3H^2} - F_R + \frac{RF_R - F}{6H^2}\right). \tag{6}$$

Here, we are considering a particular model of $F(R)$ gravity, given by:

$$F(R) = R - 2\Lambda\left(1 - e^{-\beta\mathcal{R}^\alpha}\right), \quad \mathcal{R} = \frac{R}{2\Lambda}, \tag{7}$$

where β is a dimensionless parameter and $\mathcal{R}$ is the normalized Ricci scalar. As shown in some previous literature, an additional term F_{inf} might be considered in the action (7), which would correspond to the dominated term during inflation [29]. However, such inflationary contribution is considered to become negligible at late-times, such that is not considered in this paper. Note also that by setting $\alpha = 1$ in (7), one recovers the well-known exponential $F(R)$ gravity that has been considered in previous literature [18,24–26,29]. In addition, for $\alpha > 0$ the model (7) reduces to the usual ΛCDM model for the limits $\beta \to +\infty$ and/or $R \to +\infty$, where the latter turns out at early times. In this sense, the analysis of this paper considers observational data (see Sect. 3 for more details) for late times, since the earliest data comes from the Cosmic Microwave Background (CMB), which is located at redshifts $z \simeq 1100$. Other observational data, as SN Ia, CC and BAO, are located at much less redshifts $z \leq 2.4$. The epoch with redshifts $z < 10^4$ corresponds to $\mathcal{R} < 10^{13}$ when any inflationary term F_{inf} becomes negligible, since the normalised Ricci scalar at the end of inflation is many orders of magnitude larger, $\mathcal{R}_0 \sim 10^{85}$ [47]. During the matter domination epoch at $z < 10^4$, pressureless matter contains baryons and dark matter: $\rho_m = \rho_b + \rho_{dm}$. Then, cosmological evolution for the matter and radiation energy densities are obtained by the continuity equation, which yield: (4):

$$\rho = \rho_m^0 a^{-3} + \rho_r^0 a^{-4}, \tag{8}$$

where ρ_m^0 and ρ_r^0 are the energy densities at the present time t_0, where $a(t_0) = 1$. In order to reduce the number of free parameters, the radiation-matter ratio is fixed by Planck data [33,47,48] as:

$$X_r = \frac{\rho_r^0}{\rho_m^0} = 2.9656 \cdot 10^{-4} \,. \tag{9}$$

As pointed above, for the limit $R \to +\infty$ or more precisely, for $\beta\mathcal{R}^\alpha \gg 1$, the model (7) becomes close to ΛCDM model, such that one can assume with no loss of generality that the Hubble parameter and the Ricci scalar would be close to the ones given for the ΛCDM model asymptotically, which are given by: [29,33,47]:

$$\frac{H^2}{H_0^{*2}} = \Omega_m^*\left(a^{-3} + X_r a^{-4}\right) + \Omega_\Lambda^* \,, \quad \frac{R}{2\Lambda} = 2 + \frac{\Omega_m^*}{2\Omega_\Lambda^*} a^{-3} \,. \tag{10}$$

Here H_0^*, Ω_m^* and Ω_Λ^* are the Hubble constant, matter/Λ cosmological parameters for the ΛCDM model that mimics the exponential $F(R)$ model at asymptotically at early times. Nevertheless, in general, the values for the cosmological parameters will differ for the $F(R)$ gravity model (7), since even under the assumption that the $F(R)$ model matches (10) at high redshifts $10^3 \leq z \leq 10^5$, the late-time evolution will deviate from the ΛCDM scenario. In this sense, the parameters for both models are related as follows [33]:

$$\Omega_m^0 H_0^2 = \Omega_m^*(H_0^*)^2 = \frac{\kappa^2}{3}\rho_m(t_0),$$
$$\Omega_\Lambda H_0^2 = \Omega_\Lambda^*(H_0^*)^2 = \frac{\Lambda}{3}. \tag{11}$$

Then, by using H_0^*, the Hubble parameter can be normalised as $E = \frac{H}{H_0^*}$. Whereas the dynamical equations (5) and (6) can be expressed in terms of the dimensionless variables $E(a)$ and $\mathcal{R}(a)$, which lead to:

$$\frac{dE}{dx} = \Omega_\Lambda^* \frac{\mathcal{R}}{E} - 2E, \quad x = \log a, \tag{12}$$

$$\frac{d\mathcal{R}}{dx} = \frac{\left[\Omega_m^*(a^{-3} + X_r a^{-4}) + \Omega_\Lambda^*\left(1 - (1 + \alpha\beta\mathcal{R}^\alpha)\, e^{-\beta\mathcal{R}^\alpha}\right)\right] \Big/ E^2 - 1 + \alpha\beta\mathcal{R}^{\alpha-1} e^{-\beta\mathcal{R}^\alpha}}{\alpha\beta(\alpha\beta\mathcal{R}^\alpha + 1 - \alpha)\,\mathcal{R}^{\alpha-2} e^{-\beta\mathcal{R}^\alpha}}. \tag{13}$$

By following some previous analysis (see for instance [29,33]) the system of Eqs. (12), (13) can be solved numerically by starting at some appropriate initial redshift where the ΛCDM asymptotical conditions (10) hold, which are then imposed as initial conditions for the equations. This means that at the initial point the factor $\epsilon = e^{-\beta\mathcal{R}_{\text{ini}}^\alpha}$ should be much smaller than unity. For the calculations of this paper, $\epsilon \sim 10^{-9}$ is assumed, which can be used to obtain the integration starting point through Eq. (10), which gives:

$$x_{\text{ini}} = -\frac{1}{3}\log\left\{\frac{2\Omega_\Lambda^*}{\Omega_m^*}\left[\left(\frac{\log\epsilon^{-1}}{\beta}\right)^{1/\alpha} - 2\right]\right\}. \tag{14}$$

Thus, the solutions $E(a)$, $\mathcal{R}(a)$ can be obtained for the particular $F(R)$ model that is considered here, while the Hubble parameter $H(a)$ or $H(z)$ is obtained via Eq. (11). Remind that $z = a^{-1} - 1$ and $a(t_0) = 1$. Hence, the cosmological evolution for this $F(R)$ model can be compared with observational data, which is described in the next section.

3 Observational data

In order to fit the model (7) with observational data, Supernovae Ia (SNe Ia), baryon acoustic oscillations (BAO), estimations of the Hubble parameter $H(z)$ or Cosmic Chronometers (CC) and parameters from the cosmic microwave background radiation (CMB) are considered.

In this paper, the Pantheon+ sample database [10] is used, which provides $N_{\rm SN} = 1701$ datapoints that contains information of the distance moduli $\mu_i^{\rm obs}$ at redshifts z_i from 1550 spectroscopically SNe Ia. Then, the χ^2 function is computed:

$$\chi^2_{\rm SN}(\theta_1, \dots) = \min_{H_0} \sum_{i,j=1}^{N_{\rm SN}} \Delta\mu_i \left(C_{\rm SN}^{-1}\right)_{ij} \Delta\mu_j$$
$$\Delta\mu_i = \mu^{\rm th}(z_i, \theta_1, \dots) - \mu_i^{\rm obs}. \quad (15)$$

Here θ_j are free model parameters, $C_{\rm SN}$ is the $N_{\rm SN} \times N_{\rm SN}$ covariance matrix and $\mu^{\rm th}$ are the theoretical values for the distance moduli, which is calculated as follows:

$$\mu^{\rm th}(z) = 5\log_{10}\frac{(1+z)\,D_M(z)}{10{\rm pc}}, \quad D_M(z) = c\int_0^z \frac{d\tilde{z}}{H(\tilde{z})}. \quad (16)$$

For evaluating the function (15), the Hubble constant H_0 (or equivalently the "asymptotical" constant H_0^*) is considered as a nuisance parameter.

For BAO new data from Dark Energy Spectroscopic Instrument (DESI) Data Release 1 [7–9] is considered. The comparison is performed by calculating two distances:

$$d_z(z) = \frac{r_s(z_d)}{D_V(z)}, \quad A(z) = \frac{H_0\sqrt{\Omega_m^0}}{cz} D_V(z), \quad (17)$$

where $D_V(z) = \left[cz D_M^2(z)/H(z)\right]^{1/3}$, z_d being the redshift at the end of the baryon drag era whereas the comoving sound horizon $r_s(z)$ is obtained as follows: [33]:

$$r_s(z) = \int_z^\infty \frac{c_s(\tilde{z})}{H(\tilde{z})}\, d\tilde{z}$$
$$= \frac{1}{\sqrt{3}}\int_0^{1/(1+z)} \frac{da}{a^2 H(a)\sqrt{1+\left[3\Omega_b^0/(4\Omega_\gamma^0)\right]a}}. \quad (18)$$

The estimations for z_d and for the ratio of baryons and photons Ω_b^0/Ω_γ are fixed by the Planck 2018 data [49].

DESI DR1 data [7–9] that includes BAO data from clustering of galaxies, quasars and the Lyman-α forest in the redshift range $0.1 < z < 4.16$ provides 6 datapoints, shown in Table 1. In addition, another 21 BAO data points that provide $d_z(z)$ as well as 7 data points that gives $A(z)$ are considered [33,47,50]. Then, the following χ^2 function is obtained for the fittings with BAO data:

$$\chi^2_{\rm BAO}(\Omega_m^0, \theta_1, \dots) = \Delta d \cdot C_d^{-1}(\Delta d)^T + \Delta A \cdot C_A^{-1}(\Delta A)^T. \quad (19)$$

Here, $\Delta d_i = d_z^{\rm obs}(z_i) - d_z^{\rm th}(z_i, \dots)$, $\Delta A_i = A^{\rm obs}(z_i) - A^{\rm th}(z_i, \dots)$, C_d and C_A are the covariance matrices for the correlated BAO data [51,52].

Moreover, Cosmic Chronometers (CC) or the Hubble parameter data $H(z)$, which are measured as $H(z) = \frac{\dot{a}}{a} \simeq -\frac{1}{1+z}\frac{\Delta z}{\Delta t}$ from differential ages Δt of galaxies with known Δz are considered, which provides $N_H = 32$ CC datapoints [53–60]. The χ^2 function for CC $H(z)$ data is:

$$\chi^2_H(\theta_1, \dots) = \sum_{j=1}^{N_H}\left[\frac{H(z_j, \theta_1, \dots) - H^{obs}(z_j)}{\sigma_j}\right]^2. \quad (20)$$

Regarding the CMB observational parameters from Planck 2018 data [49], the following values are considered [61]:

$$R = \sqrt{\Omega_m^0}\frac{H_0 D_M(z_*)}{c}, \quad \ell_A = \frac{\pi D_M(z_*)}{r_s(z_*)}, \quad \omega_b = \Omega_b^0 h^2, \quad (21)$$

where z_* is the photon-decoupling redshift estimated in Ref. [61], D_M is the comoving distance (16), $h = H_0/[100\,{\rm km s^{-1} Mpc^{-1}}]$ and $r_s(z)$ is the comoving sound horizon (18). The corresponding χ^2 function for the CMB data is computed by:

$$\chi^2_{\rm CMB} = \min_{\omega_b} \Delta\mathbf{x} \cdot C_{\rm CMB}^{-1}\left(\Delta\mathbf{x}\right)^T, \quad \Delta\mathbf{x} = \mathbf{x} - \mathbf{x}^{Pl} \quad (22)$$

where $\mathbf{x} = \left(R, \ell_A, \omega_b\right)$. The observational values, which are obtained with free amplitude for the lensing power spectrum, are provided in [49,61].

$$\mathbf{x}^{Pl} = \left(1.7428 \pm 0.0053,\ 301.406 \pm 0.090,\ 0.02259 \pm 0.00017\right). \quad (23)$$

The covariance matrix $C_{\rm CMB} = \|\tilde{C}_{ij}\sigma_i\sigma_j\|$ is described in Ref. [61].

In the following section, the model (7) and the ΛCDM model are compared by using the above observational data sources and the corresponding fits for the free parameters are obtained.

Table 1 DESI DR1 BAO data

z_{eff}	0.295	0.51	0.706	0.93	1.317	2.33
z range	0.1–0.4	0.4–0.6	0.5–0.8	0.8–1.1	1.1–1.6	1.77–4.16
d_z	0.1261 ± 0.0024	0.0796 ± 0.0018	0.0629 ± 0.0014	0.05034 ± 0.0008	0.04144 ± 0.0011	0.03173 ± 0.00073

4 Testing the models with observational data

The $F(R)$ model (7) is compared to the above observational data. To do so, two cases are considered: fixing $\alpha = 1$ and keeping α as a free parameter its observational predictions. For this purpose, the total χ^2 function with the contributions from SN Ia, BAO, CC and CMB is computed:

$$\chi^2 = \chi^2_{\text{SN}} + \chi^2_{\text{BAO}} + \chi^2_H + \chi^2_{\text{CMB}} \,. \tag{24}$$

The model (7), after fixing the radiation-matter ratio (9), contains $N_p = 5$ free parameters:

$$\alpha, \quad \beta, \quad \Omega^0_m, \quad \Omega_\Lambda, \quad H_0 \,. \tag{25}$$

For $\alpha = 1$, that recovers the standard exponential gravity model, the number of free parameters is reduced to $N_p = 4$. In both scenarios the fittings are computed for the parameters Ω^0_m, Ω_Λ, H_0 instead of Ω^*_m, Ω^*_Λ, H^*_0, by using the relations (11).

The results for both exponential cases are depicted in Fig. 1, where the ΛCDM model is also included for comparison, which is described by the Hubble parameter:

$$H^2 = H_0^2\big[\Omega^0_m(a^{-3} + X_r a^{-4}) + 1 - \Omega^0_m - \Omega^0_r\big], \tag{26}$$

which contains $N_p = 2$ free parameters Ω^0_m and H_0. Note that the ΛCDM scenario is recovered in the limit $\beta \to +\infty$ for the model (7) independently of $\alpha > 0$.

In order to show the results of the fits for the free parameters (25), the corresponding contour plots are depicted in Fig. 1. The contours correspond to 1σ (68.27%) and 2σ (95.45%) confidence regions for the two-parameter distributions $\chi^2(\theta_i, \theta_j)$, which are obtained by minimising the χ^2 over all the remaining free parameters. For instance, the contours depicted in the bottom-left panel of Fig. 1 are obtained by

$$\chi^2(\Omega^0_m, H_0) = \min_{\alpha,\beta,\Omega_\Lambda} \chi^2(\alpha, \ldots, H_0),$$

and show the estimations for the three models.

The blue stars for the $F(R)$ model (7), the magenta diamonds for the case $\alpha = 1$ and the green circles for ΛCDM denote the best fits with min χ^2 of the corresponding two-dimensional distributions. The best fits for the free parameters are also shown in Fig. 1 in the one-parameter distributions $\chi^2(H_0)$ and the likelihoods $\mathcal{L}(\theta_j)$, which are obtained by:

$$\mathcal{L}(\theta_j) = \exp\left[-\frac{\chi^2(\theta_j) - m^{\text{abs}}}{2}\right], \tag{27}$$

where $\chi^2(\theta_j) = \min_{\text{other } \theta_k} \chi^2(\theta_1, \ldots)$, θ_j is the corresponding model parameter and m^{abs} the absolute minimum for χ^2. In addition, the best fits with the corresponding 1σ errors for the free model parameters (25) are also shown explicitly in Table 2 below.

As shown in Table 2, the generalized exponential $F(R)$ model (7) with provides a best fit for α that is very close to 1, in other words, for the above observational data, the generalized model (7) achieves the best results when it becomes the standard exponential $F(R)$ model (7) with $\alpha = 1$. In addition, both cases show the same absolute value for the min χ^2.

The one-parameter distributions $\chi^2(H_0)$ for all the models are shown in the top-right panel of Fig. 1. The results seem to favour clearly the modified gravity models in comparison to the ΛCDM model. One may conclude that the last Pantheon+ SN Ia and DESI BAO observational data change the domain of the free parameters, where both exponential $F(R)$ models achieve the most successful results, in comparison to previous analysis in the literature [29]. The fits for the parameter β favours smaller values than previous analysis with older data. The main point lies on the fact that the smaller β values are, the larger the difference between exponential $F(R)$ models and the ΛCDM arise, which is reflected in the different values for χ^2 for each model. By considering larger β values, the χ^2 in the $F(R)$ cases become larger and tend to the ΛCDM results.

In addition, the different behaviour of the exponential $F(R)$ models in comparison to the ΛCDM scenario also leads to different predictions for the best fits of the Hubble constant H_0 and for the matter density parameter Ω^0_m. Table 2 shows that the ΛCDM best fit of the Hubble constant is given by $H_0 = 68.51^{+1.56}_{-1.53}$ km/(s·Mpc) whereas for the model (7), it leads to $H_0 = 66.06^{+1.61}_{-1.59}$ km/(s·Mpc) (the case $\alpha = 1$ provides similar result), which are mutually excluded at 1σ. For the matter density parameter Ω^0_m the ΛCDM and $F(R)$ models are excluded to more than 3σ in their predictions, as shown in Fig. 1.

The best fits for β and Ω_Λ are rather close for both exponential models, in particular, $\Omega_\Lambda = 0.571^{+0.058}_{-0.057}$ for model

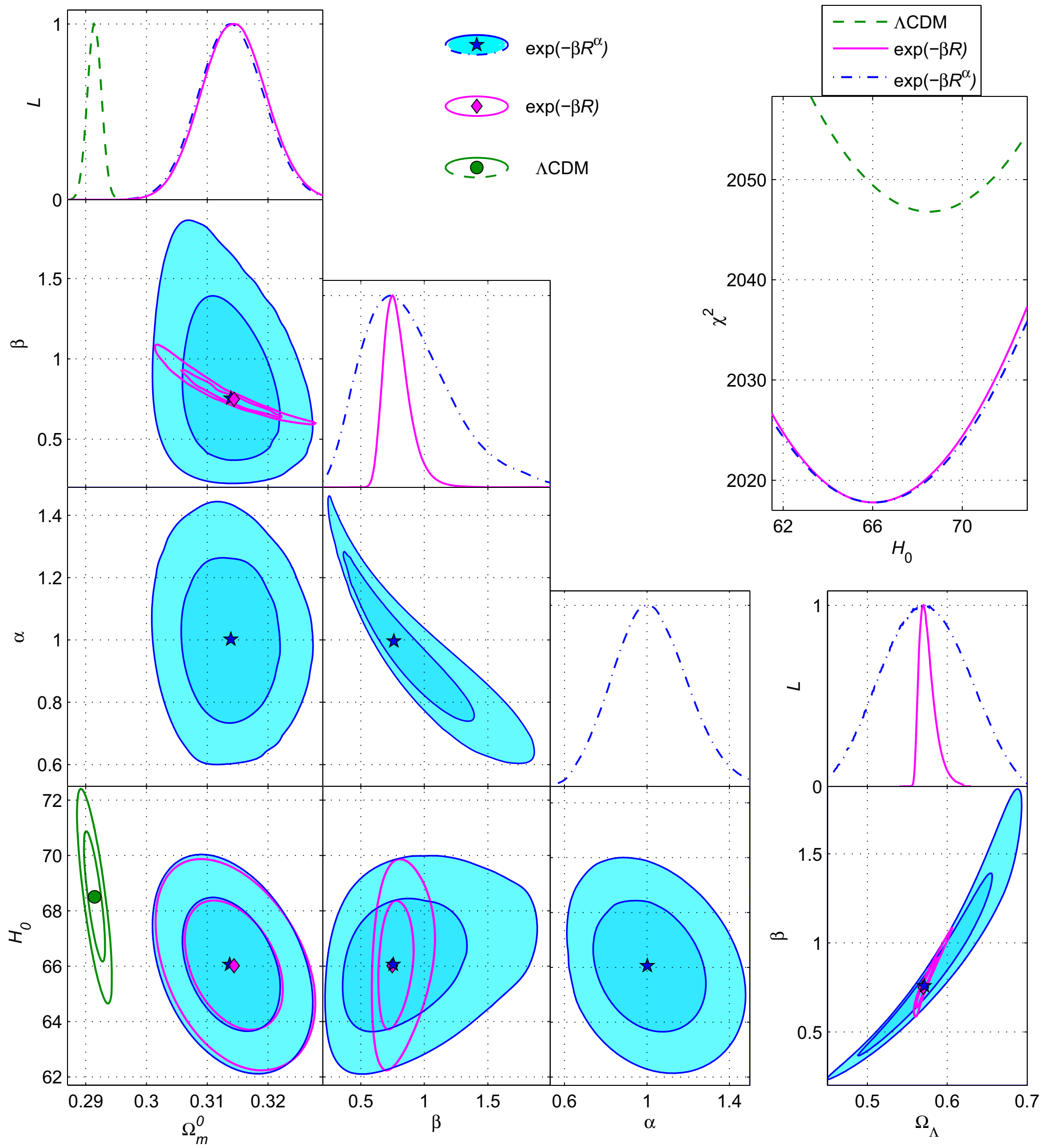

Fig. 1 Contour plots of χ^2 with 1σ, 2σ CL, likelihood functions $\mathcal{L}(\theta_i)$ and one-parameter distributions $\chi^2(H_0)$ for the exponential $F(R)$ model (7) in comparison with its particular case $\alpha = 1$ and with the ΛCDM model

(7) and $\Omega_\Lambda = 0.570^{+0.010}_{-0.007}$ for its case $\alpha = 1$. For the scenario (7), the 1σ error are larger (and the contours are wider) that may be connected with the additional degree of freedom α, though the best fit for α is close to 1. However, they both lead to similar best fits for H_0 and Ω_m^0.

The large difference regarding the best fits for both exponential models when comparing the absolute minimum $m^{\text{abs}} = \min \chi^2$ with respect to the standard ΛCDM model does not vanish even when considering the number of free parameters N_p for each case and following the Akaike information criterion [62]

$$\text{AIC} = \min \chi^2_{tot} + 2N_p. \tag{28}$$

The more free parameters has a model, the larger AIC is. As shown in Table 2, despite $2N_p$ is smaller for the ΛCDM model, this does not save the standard model of cosmology in comparison to the exponential modified gravity. To show this clearer, the difference $\Delta\text{AIC} = \text{AIC}_{\text{model}} - \text{AIC}_{\Lambda\text{CDM}}$ is included in Table 2.

5 Parameterisations of the dark energy EoS

Previous results concerning the great success of the exponential $F(R)$ models in comparison to ΛCDM model when considering the Akaike information criterion suggests two key questions: (a) what is the nature of the large differences according to ΔAIC, are any of the observational data strongly favouring modified gravity in comparison to others?; (b) are those results pointing to a dynamical EoS parameter for dark energy? The last question is also inspired by recent attempts [7,38–40] to confront the last DESI BAO data with different scenarios.

In this section, we test two popular parameterisations of EoS for dark energy: the so-called wCDM model and the Chevallier–Polarski–Linder (CPL or $w_0 w_a$CDM) model [36, 37]. The pressure and energy densities of dark energy are related by its EoS

$$p_{\rm de} = w\rho_{\rm de},$$

where,

$$w = \text{const}, \quad \text{for} \quad w-\text{CDM model},$$
$$w = w_0 + w_1(1-a), \quad \text{for CPL model.} \tag{29}$$

Both provide a generalisation of ΛCDM model in an agnostic model way. Then, the Hubble parameter yields:

$$H^2 = H_0^2\big[\Omega_m^0(a^{-3}+X_r a^{-4})+(1-\Omega_m^0-\Omega_r^0)\,f(a)\big], \tag{30}$$

where $f(a) = a^{-3(1+w)}$ for wCDM and $f(a) = a^{-3(1+w_0+w_1)}e^{3w_1(a-1)}$ for CPL model. By comparing to ΛCDM model, one can see that an additional parameter w arises in wCDM while CPL model contains two extra free parameters, w_0, w_1. For $w_1 = 0$ CPL reduces to wCDM whereas ΛCDM model is recovered for $w = w_0 = -1$ in both cases (together with $w_1 = 0$ in the CPL model).

Results of the comparison with observational data for these models are shown in Table 2 and depicted in Fig. 2. For wCDM model the absolute minimum of χ^2, the value for AIC (28) and the best fits for Ω_m^0 and H_0 lies in-between the ΛCDM and $F(R)$ results, whereas data again strongly favours the CPL scenario, where the min χ^2 and AIC parameter achieve the smallest values.

As shown in Table 2, the best fits of Ω_m^0 and H_0 for the CPL model and exponential $F(R)$ gravities are very close, such that the CPL best fits also differs with respect to the ΛCDM predictions for more than 3σ in the case of the density parameter Ω_m^0 and near 1σ for H_0.

According to min χ^2 and the Akaike information criterion, CPL fits slightly better the data in comparison to the standard exponential gravity model, but with no statistical significance, despite both models contain the same number of free parameters $N_p = 4$. However, this difference in AIC and ΔAIC is small in comparison with that for wCDM and ΛCDM. The generalised exponential $F(R)$ model (7) shows a worse AIC comparison with respect to standard exponential gravity and CPL model, since it contains an extra free parameter ($N_p = 5$).

The CPL best fits and min χ^2 values in Table 2 and Fig. 2 differ from the wCDM results, because the CPL best fit for w_1 is far from zero, which corresponds to wCDM model. Indeed, the smaller AIC value for the CPL model reflects a strong deviation from a constant EoS for dark energy, either wCDM or ΛCDM model. Moreover, wCDM lies in-between the CPL model and ΛCDM model concerning the goodness of the fits as provided by the AIC parameter. Also the value for the Hubble constant is close for both cases.

The question about the origin of the large deviations ΔAIC favouring the standard exponential gravity and the CPL model requires additional investigations: what type of new observational data is behind these results? It may be connected with the DESI DR1 BAO data [7–9] that are tabulated as 6 datapoints in Table 1. To understand their role, additional tests are followed for the standard exponential $F(R)$ model, wCDM, CPL and ΛCDM scenarios by considering two sets of observational data separately: (a) SN Ia, $H(z)$ or Cosmic Chronometers (CC), CMB and only 6 DESI BAO; and (b) SN Ia, CC, CMB observational data (without BAO). The results are shown in Table 3 and Fig. 3. The generalised exponential model (7) is excluded because of the large number of free parameters $N_p = 5$ that increases the AIC value in comparison to standard exponential gravity.

By analyzing the results shown in Table 3, one may conclude that the DESI BAO data can slightly shift some estimations of the model parameters, but does not affect the large difference ΔAIC between ΛCDM by one side and exponential, wCDM or CPL models by the another side. Indeed, such a difference becomes larger in absence of DESI BAO data We see that ΔAIC between the mentioned 3 scenarios do not disappear in the cases (a) and (b). Thus, the reason of large differences in ΔAIC of the exponential, wCDM and CPL scenarios lies in the SN Ia Pantheon+ data [10]. Remind that a large negative ΔAIC of the aforementioned 3 models points to a clear advantage in describing the observational data in comparison with ΛCDM.

By following the hierarchy of AIC criterion for these four models when considering the three observational datasets (with all BAO data, just with DESI BAO data and with no BAO data), shown in Tables 2 and 3, CPL model arises as the most successful one, followed by the exponential $F(R)$ model, wCDM and ΛCDM. However, these models respond differently to changes in BAO data sets. For the exponential and ΛCDM models, min χ^2 and AIC grow successively when BAO datasets are considered, while the best fits of the density parameter Ω_m^0 and the Hubble constant H_0 remain nearly the same for all three datasets, as shown in Fig. 3.

Another picture takes place for wCDM and CPL scenarios. On can see fundamental changes of the best fits for Ω_m^0 and H_0 in Fig. 3, Tables 2 and 3, where wCDM model shows a remarkable difference on the min χ^2 and AIC when DESI data is included and especially for the other BAO data.

Table 2 The best fit values for the free parameters, min χ^2, AIC and ΔAIC for the two exponential $F(R)$ models (7) in comparison with ΛCDM, wCDM and CPL models

Model	min $\chi^2/d.o.f$	AIC	ΔAIC	Ω_m^0	H_0	Other parameters
Exp. Grav. $e^{-\beta\mathcal{R}^\alpha}$	2017.80 /1766	2027.80	-22.99	$0.3138^{+0.0054}_{-0.0052}$	$66.06^{+1.61}_{-1.59}$	$\beta=0.733^{+0.377}_{-0.273}$, $\alpha=1.002^{+0.184}_{-0.173}$
Exp. Grav. $e^{-\beta\mathcal{R}}$	2017.80 /1767	2025.80	-24.99	$0.3144^{+0.0053}_{-0.0055}$	$66.02^{+1.57}_{-1.53}$	$\beta=0.750^{+0.099}_{-0.079}$
ΛCDM	2046.79 /1769	2050.79	0	$0.2914^{+0.0012}_{-0.0011}$	$68.51^{+1.56}_{-1.53}$	–
wCDM	2029.93 /1768	2035.93	-14.86	$0.3108^{+0.0050}_{-0.0050}$	$67.97^{+1.53}_{-1.53}$	$w=-0.926^{+0.018}_{-0.018}$
CPL	2015.72 /1767	2023.72	-27.07	$0.3153^{+0.0053}_{-0.0053}$	$66.03^{+1.59}_{-1.58}$	$w_0=-0.741^{+0.054}_{-0.053}$, $w_1=-0.635^{+0.175}_{-0.183}$

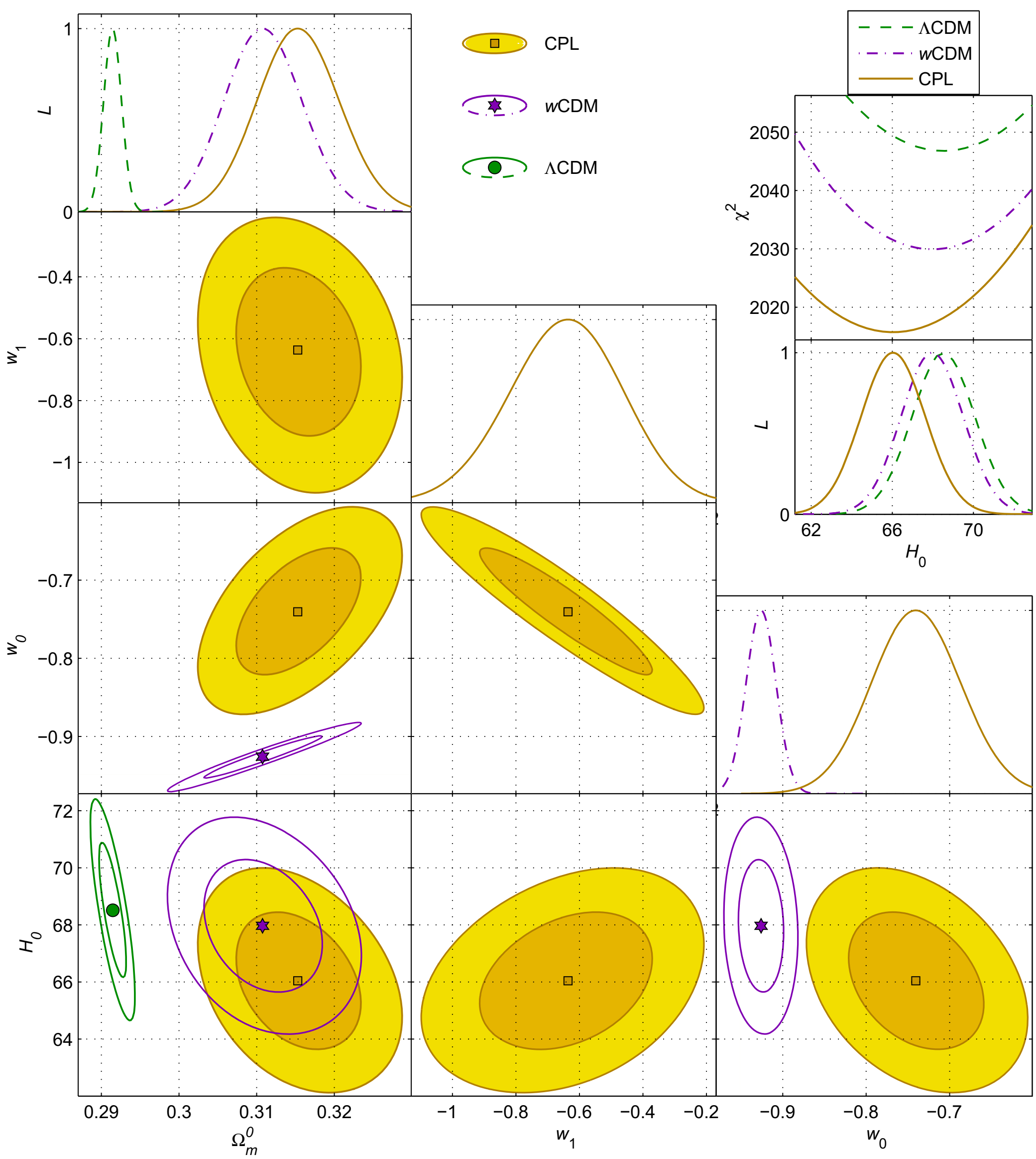

Fig. 2 Contour plots of χ^2 with 1σ, 2σ CL, likelihoods $\mathcal{L}(\theta_i)$ and one-parameter distributions $\chi^2(H_0)$ for the wCDM and CPL scenarios in comparison with the ΛCDM model

Table 3 The best fits, min χ^2, AIC and ΔAIC for observational data (a) with only 6 DESI BAO datapoints and (b) without BAO data for the exponential $F(R)$ gravity, ΛCDM, wCDM and CPL models

Data	(a) SN Ia + CC + CMB + 6 DESI BAO datapoints					(b) SN Ia + CC + CMB				
Model	Min$\chi^2/d.o.f$	AIC	ΔAIC	Ω_m^0	H_0	Minχ^2	AIC	ΔAIC	Ω_m^0	H_0
Exp $e^{-\beta\mathcal{R}}$	2000.32 /1746	2008.32	− 27.83	$0.3158^{+0.0061}_{-0.0058}$	$66.05^{+1.58}_{-1.63}$	1997.98	2005.98	− 28.24	$0.3156^{+0.0061}_{-0.0060}$	$66.21^{+1.63}_{-1.63}$
ΛCDM	2032.15 /1748	2036.15	0	$0.2913^{+0.0012}_{-0.0012}$	$68.60^{+1.62}_{-1.59}$	2030.22	2034.22	0	$0.2912^{+0.0012}_{-0.0012}$	$68.72^{+1.64}_{-1.60}$
wCDM	2005.44 /1747	2011.44	− 24.71	$0.3256^{+0.0074}_{-0.0072}$	$66.22^{+1.61}_{-1.61}$	2001.59	2007.59	− 26.63	$0.3300^{+0.0083}_{-0.0079}$	$65.74^{+1.64}_{-1.60}$
CPL	1998.82 /1746	2006.82	− 29.33	$0.3155^{+0.0080}_{-0.0077}$	$65.99^{+1.61}_{-1.61}$	1995.68	2003.68	− 30.54	$0.3068^{+0.0110}_{-0.0101}$	$66.43^{+1.71}_{-1.63}$

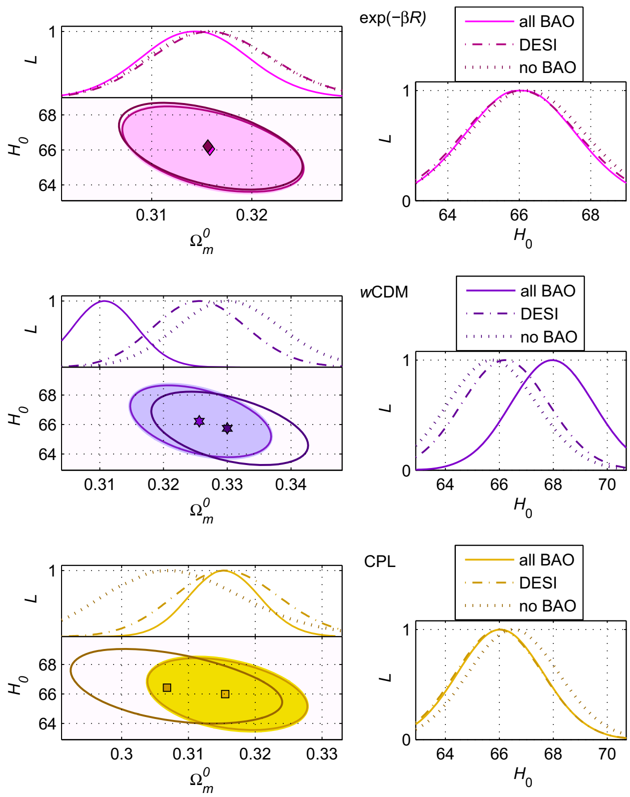

Fig. 3 Comparison of 1σ contour plots and likelihoods for the exponential $F(R)$, wCDM, ΛCDM and CPL scenarios, filled and empty contours correspond to only DESI and without BAO data respectively

The corresponding changes of AIC for wCDM from − 26.63 (without BAO data) to − 14.86 (with BAO data) are essentially larger than for the other models. One also can see that the best fits for Ω_m^0 for the wCDM model leads to important differences when BAO data is included (while the best fit for H_0 grow). The parameters distributions for the CPL model also differs from one dataset to another but with smaller deviations, whereas exponential gravity points to the same fits independently of the BAO datasets.

6 Conclusions

As shown in previous literature, exponential $F(R)$ gravities have been widely studied, since they show an ability to reproduce well the whole cosmological evolution, including GR predictions at both early as late times, and at the same time they are constructed in such a way that pass local scale constraints [18,29].

In this paper, exponential $F(R)$ gravity is reconsidered and confronted to the latest observational data, including Pantheon+ SN Ia, new BAO data from DESI DR1, the Hubble parameter CC estimations and CMB data. To do a reliable test with the aforementioned observational data, a generalised exponential gravity model is also considered to check deviations from standard exponential gravity. Both models are then compared with the fits and predictions of the standard ΛCDM model and also to wCDM and CPL models [36,37].

To do the fits, the usual technique of the minimum χ^2 is followed. The best fits for these scenarios are summarised in Table 2 and also shown in Figs. 1 and 2. As one can see, both exponential gravity models show a much better accuracy while fitting the observational data than ΛCDM model, as indicated by a much smaller min χ^2. Moreover, even if one considers the extra free parameters of the modified gravity models as an artificial handmade way to get better fits, the observational data still favours clearly these models to the detriment of ΛCDM model. Indeed, when computing the AIC coefficient which penalise the number of free parameters, results still support strongly the modified gravity scenario. In addition, the fits of the generalised exponential gravity model points towards the standard exponential gravity case, since the extra parameter is centred in $\alpha = 1$, which recovers the usual exponential gravity model. In addition, the standard exponential gravity model is also strongly supported in comparison with wCDM model, but slightly below the CPL model with the observational data.

In fact, previous analysis of the same exponential gravity model favoured ΛCDM, as shown in Ref. [29], where the results led to a value for the fundamental parameter given by $\beta = 2.38^{+\infty}_{-0.8}$. Recalling that ΛCDM is recovered for $\beta \to \infty$, those previous results were clearly pointing out to ΛCDM model, which was included within 1σ confidence region for β. Here, we have shown that this is not the case for the last available observational data, where one obtains $\beta = 0.75^{+0.099}_{-0.079}$ for the standard exponential gravity model ($\alpha = 1$) and $\beta = 0.733^{+0.377}_{-0.273}$ for the generalised model, both given by (7). For the former, ΛCDM turns out excluded at 4σ. In addition, in order to get a strong confidence on these results, we have computed the min χ^2 by fixing the β parameter to larger and larger values, which at the end tend to the min χ^2 of ΛCDM results. From Table 2 and Fig. 1, one can also infer that the best fits for the parameters H_0 and Ω_m^0 in the exponential $F(R)$ models and in the ΛCDM scenario differ notably. In particular, our results point to an even smaller value for the Hubble constant $H_0 = 66.06^{+1.61}_{-1.59}$ km/(s·Mpc), what would increase the H_0 tension when compared with the value provided by the calibration of SNe Ia [63–65].

In addition, CPL parametrisation of the EoS parameter for dark energy also excludes ΛCDM at 4σ, while the best fit for H_0 in this scenario is also small and almost coincides with the $F(R)$ prediction. This is in agreement with previous analysis, which also pointed out to Pantheon+ catalogue as the dataset favouring dynamical dark energy [43]. The Hubble constant for the exponential gravity and CPL fits better the value provided by Planck estimations from the CMB [49]. For the matter density parameter Ω_m^0, a difference of more than 3σ arises in comparison of the ΛCDM with the $F(R)$ models and also with CPL, what results in the condition of mutually exclusive of both descriptions of the cosmological evolution. Moreover, the goodness of the fits favours clearly a dynamical EoS for dark energy, either is described by a parameterisation (CPL model) or by modified gravity.

Hence, tests with the latest observational data show a large advantage of the exponential $F(R)$ model, CPL and wCDM scenarios in comparison to ΛCDM model in terms of the minimum of χ^2 and the AIC criterion. This picture strongly differs from previous results with older observational data [29–32]. To find out the answer behind this change of paradigm, additional tests are raised for every model, where by assuming the observational data provided by SN Ia, CC and CMB, we played with the different sets of BAO data: (a) with only 6 DESI BAO datapoints and (b) without BAO data. By Analysing the results shown in Table 3 and Fig. 3, we may conclude that the the large difference in the AIC parameter between $F(R)$, CPL, wCDM models and ΛCDM scenarioa are not connected not with DESI BAO data, but with SN Ia Pantheon+ data [10].

Then, success of the exponential gravity in describing the observational datasets suggests that a more complete theory of gravity, beyond GR, might have to include non-linear terms of the Ricci scalar in the action at the cosmological limit, at least. Hence, we can conclude that the game of rivalry among modified gravities/dynamical dark energy vs ΛCDM is balanced to one side by now with the background cosmological data described above.

Acknowledgements This work was supported by MICINN (Spain) project PID2020-117301GA-I00 (D.S.G.) funded by MCIN/AEI/10.13039/501100011033 ("ERDF A way of making Europe" and "PGC Generación de Conocimiento") and also by the program Unidad de Excelencia Maria de Maeztu CEX2020-001058-M, Spain (S.D.O).

Funding Financial support of the Department of Education, Junta de Castilla y León (Spain), and FEDER Funds is also gratefully acknowledged (Reference: CLU-2023-1-05).

Data Availability Statement This manuscript has no associated data. [Author's comment: Data sharing not applicable to this article as no datasets were generated or analysed during the current study.].

Code Availability Statement This manuscript has no associated code/software. [Author's comment: Code/Software sharing not applicable to this article as no code/software was generated or analysed during the current study.].

Open Access This article is licensed under a Creative Commons Attribution 4.0 International License, which permits use, sharing, adaptation, distribution and reproduction in any medium or format, as long as you give appropriate credit to the original author(s) and the source, provide a link to the Creative Commons licence, and indicate if changes were made. The images or other third party material in this article are included in the article's Creative Commons licence, unless indicated otherwise in a credit line to the material. If material is not included in the article's Creative Commons licence and your intended use is not permitted by statutory regulation or exceeds the permitted use, you will need to obtain permission directly from the copyright holder. To view a copy of this licence, visit http://creativecommons.org/licenses/by/4.0/.
Funded by SCOAP^3.

References

1. S. Capozziello, M. De Laurentis, Phys. Rep. **509**, 167 (2011). arXiv:1108.6266 [gr-qc]
2. S. Nojiri, S.D. Odintsov, V.K. Oikonomou, Phys. Rep. **692**, 1 (2017). arXiv:1705.11098
3. S. Nojiri, S.D. Odintsov, Phys. Rep. **505**, 59 (2011). arXiv:1011.0544 [gr-qc]
4. V. Faraoni, S. Capozziello, *Beyond Einstein Gravity: A Survey of Gravitational Theories for Cosmology and Astrophysics* (Springer, 2011)
5. A. de la Cruz-Dombriz, D. Saez-Gomez, Entropy **14**, 1717 (2012). arXiv:1207.2663 [gr-qc]
6. S.D. Odintsov, V.K. Oikonomou, I. Giannakoudi, F.P. Fronimos, E.C. Lymperiadou, Symmetry **15**(9), 1701 (2023). arXiv:2307.16308 [gr-qc]
7. DESI Collaboration, A.G. Adame et al. [DESI], arXiv:2404.03002 [astro-ph.CO]
8. R. Calderon et al., JCAP **10**, 048 (2024). arXiv:2405.04216
9. K. Lodha et al., arXiv:2405.13588
10. D. Scolnic et al., Astrophys. J. **938**, 113 (2022). arXiv:2112.03863
11. S. Roy Choudhury, T. Okumura, arXiv:2409.13022
12. D. Batic, S.B. Medina, M. Nowakowski, arXiv:2409.19577

13. E. Di Valentino, O. Mena, S. Pan, L. Visinelli, W. Yang, A. Melchiorri, D.F. Mota, A.G. Riess, J. Silk, Class. Quantum Gravity **38**(15), 153001 (2021). https://doi.org/10.1088/1361-6382/ac086d. arXiv:2103.01183 [astro-ph.CO]
14. S. Vagnozzi, Universe **9**(9), 393 (2023). https://doi.org/10.3390/universe9090393. arXiv:2308.16628 [astro-ph.CO]
15. F. Bajardi, R. D'Agostino, M. Benetti, V. De Falco, S. Capozziello, Eur. Phys. J. Plus **137**(11), 1239 (2022). arXiv:2211.06268 [gr-qc]
16. W. Hu, I. Sawicki, Phys. Rev. D **76**, 064004 (2007). https://doi.org/10.1103/PhysRevD.76.064004. arXiv:0705.1158 [astro-ph]
17. S. Nojiri, S.D. Odintsov, Phys. Rev. D **77**, 026007 (2008). https://doi.org/10.1103/PhysRevD.77.026007. arXiv:0710.1738 [hep-th]
18. E.V. Linder, Phys. Rev. D **80**, 123528 (2009). arXiv:0905.2962
19. S.A. Appleby, R.A. Battye, Phys. Lett. B **654**, 7 (2007). arXiv:0705.3199 [astro-ph]
20. D. Saez-Gomez, Class. Quantum Gravity **30**, 095008 (2013). arXiv:1207.5472 [gr-qc]
21. A. de la Cruz-Dombriz, P.K.S. Dunsby, S. Kandhai, D. Saez-Gomez, Phys. Rev. D **93**(8), 084016 (2016). arXiv:1511.00102 [gr-qc]
22. K. Ravi, A. Chatterjee, B. Jana, A. Bandyopadhyay, Mon. Not. R. Astron. Soc. **527**(3), 7626–7651 (2024). arXiv:2306.12585 [astro-ph.CO]
23. A. Oliveros, M.A. Acero, Phys. Dark Univ. **40**, 101207 (2023). arXiv:2302.07022 [gr-qc]
24. G. Cognola, E. Elizalde, S. Nojiri, S.D. Odintsov, L. Sebastiani, S. Zerbini, Phys. Rev. D **77**, 046009 (2008). arXiv:0712.4017 [hep-th]
25. E. Elizalde, S. Nojiri, S.D. Odintsov, L. Sebastiani, S. Zerbini, Phys. Rev. D **83**, 086006 (2011). arXiv:1012.2280 [hep-th]
26. K. Bamba, C.Q. Geng, C.C. Lee, JCAP **1008**, 021 (2010). arXiv:1005.4574
27. L. Yang, C.C. Lee, L.W. Luo, C.Q. Geng, Phys. Rev. D **82**, 103515 (2010). arXiv:1010.2058
28. Y. Chen, C.-Q. Geng, C.-C. Lee, L.-W. Luo, Z.-H. Zhu, Phys. Rev. D **91**, 044019 (2015). arXiv:1407.4303
29. S.D. Odintsov, D. Saez-Chillon Gomez, G.S. Sharov, Eur. Phys. J. C **77**, 862 (2017). arXiv:1709.06800
30. S.D. Odintsov, D. Sáez-Chillón Gómez, G.S. Sharov, Nucl. Phys. B **966**, 115377 (2021). arXiv:2011.03957
31. S.D. Odintsov, V.K. Oikonomou, L. Sebastiani, Nucl. Phys. B **923**, 608 (2017). arXiv:1708.08346 [gr-qc]
32. S.D. Odintsov, D. Saez-Chillon Gomez, G.S. Sharov, Phys. Rev. D **99**, 024003 (2019). arXiv:1807.02163
33. S.D. Odintsov, D. Sáez-Chillón Gómez, G.S. Sharov, Phys. Dark Univ. **42**, 101369 (2023). arXiv:2310.20302 [gr-qc]
34. L.N. Granda, Eur. Phys. J. C **80**(6), 539 (2020). arXiv:2003.09006
35. V.K. Oikonomou, Phys. Rev. D **103**(12), 124028 (2021). arXiv:2012.01312 [gr-qc]
36. M. Chevallier, D. Polarski, Int. J. Mod. Phys. D **10**, 213 (2001). arXiv:gr-qc/0009008
37. E.V. Linder, Phys. Rev. Lett. **90**, 091301 (2003). arXiv:astro-ph/0208512
38. A. Chudaykin, M. Kunz, arXiv:2407.02558 [astro-ph.CO]
39. C.G. Park, J. de Cruz Perez, B. Ratra, arXiv:2410.13627 [astro-ph.CO]
40. A. Notari, M. Redi, A. Tesi, arXiv:2411.11685 [astro-ph.CO]
41. B.R. Dinda, JCAP **09**, 062 (2024). https://doi.org/10.1088/1475-7516/2024/09/062. arXiv:2405.06618 [astro-ph.CO]
42. I.D. Gialamas, G. Hütsi, K. Kannike, A. Racioppi, M. Raidal, M. Vasar, H. Veermäe, arXiv:2406.07533 [astro-ph.CO]
43. B.R. Dinda, R. Maartens, arXiv:2407.17252 [astro-ph.CO]
44. R.C. Nunes, S. Pan, E.N. Saridakis, JCAP **08**, 011 (2016). https://doi.org/10.1088/1475-7516/2016/08/011. arXiv:1606.04359 [gr-qc]
45. E. Di Valentino, A. Melchiorri, J. Silk, Astrophys. J. Lett. **908**(1), L9 (2021). https://doi.org/10.3847/2041-8213/abe1c4. arXiv:2003.04935 [astro-ph.CO]
46. L.A. Escamilla, W. Giarè, E. Di Valentino, R.C. Nunes, S. Vagnozzi, JCAP **05**, 091 (2024). https://doi.org/10.1088/1475-7516/2024/05/091. arXiv:2307.14802 [astro-ph.CO]
47. S.D. Odintsov, D. Sáez-Chillón Gómez, G.S. Sharov, Phys. Dark Univ. **46**, 101558 (2024). arXiv:2406.08831 [gr-qc]
48. Planck Collaboration, P.A.R. Ade et al., Astron. Astrophys. **571**, A16 (2014). arXiv:1303.5076
49. Planck Collaboration, N. Aghanim et al., Astron. Astrophys. **641**, A6 (2020). arXiv:1807.06209
50. S.D. Odintsov, V.K. Oikonomou, G.S. Sharov, Phys. Lett. B **843**, 137988 (2023). arXiv:2305.17513
51. W.J. Percival et al., Mon. Not. R. Astron. Soc. **401**, 2148 (2010). arXiv:0907.1660
52. C. Blake et al., Mon. Not. R. Astron. Soc. **418**, 1707 (2011). arXiv:1108.2635
53. J. Simon, L. Verde, R. Jimenez, Phys. Rev. D **71**, 123001 (2005). arXiv:astro-ph/0412269
54. D. Stern, R. Jimenez, L. Verde, M. Kamionkowski, S.A. Stanford, JCAP **1002**, 008 (2010). arXiv:0907.3149
55. M. Moresco et al., JCAP **1208**, 006 (2012). arXiv:1201.3609
56. C. Zhang et al., Res. Astron. Astrophys. **14**, 1221 (2014). arXiv:1207.4541
57. M. Moresco, Mon. Not. R. Astron. Soc. **450**(1), L16 (2015). arXiv:1503.01116
58. M. Moresco et al., JCAP **1605**, 014 (2016). arXiv:1601.01701
59. A.L. Ratsimbazafy et al., Mon. Not. R. Astron. Soc. **467**(3), 3239 (2017). arXiv:1702.00418
60. N. Borghi, M. Moresco, A. Cimatti, Astrophys. J. Lett. **928**(1), L4 (2022). arXiv:2110.04304
61. L. Chen, Q.-G. Huang, K. Wang, J. Cosmol. Astropart. Phys. **1902**, 028 (2019). arXiv:1808.05724
62. H. Akaike, IEEE Trans. Autom. Control **19**, 716 (1974)
63. L. Breuval, A.G. Riess, S. Casertano et al., Astrophys. J. **973**(1), 30 (2024). arXiv:2404.08038
64. A.G. Riess, W. Yuan, L.M. Macri, D. Scolnic, D. Brout, S. Casertano, D.O. Jones, Y. Murakami, L. Breuval, T.G. Brink et al., Astrophys. J. Lett. **934**(1), L7 (2022). https://doi.org/10.3847/2041-8213/ac5c5b. arXiv:2112.04510 [astro-ph.CO]
65. D. Brout, D. Scolnic, B. Popovic, A.G. Riess, J. Zuntz, R. Kessler, A. Carr, T.M. Davis, S. Hinton, D. Jones et al., Astrophys. J. **938**(2), 110 (2022). https://doi.org/10.3847/1538-4357/ac8e04. arXiv:2202.04077 [astro-ph.CO]